1.5.7.3. *Linear magnetic birefringence*

The magnetic contribution to the component of the dielectric permittivity $\delta\varepsilon_{ij}$ can be represented as a series in the powers of the components of the magnetization and the antiferromagnetic vector. The magnetic birefringence (also called the Cotton–Mouton or Voigt effect) is described by the real symmetrical part of the tensor $\delta\varepsilon_{ij}$. In paramagnetic crystals, the magnetization $\mathbf{M}$ is proportional to the applied magnetic field $\mathbf{H}$, and the series has the form

$$\delta\varepsilon_{ij} = Q^{MM}_{ijk\ell} M_k M_\ell = Q^{MM}_{ijk\ell} \chi^M_{kr} \chi^M_{\ell s} H_r H_s = \Gamma_{ijrs} H_r H_s. \quad (1.5.7.18)$$

The tensor Γ_{ijrs} is symmetric with respect to both the first and the second pair of indices. The symmetry of this tensor implies that the diagonal components of the permittivity tensor include magnetic corrections. The modification of the diagonal components gives rise to birefringence in cubic crystals and to a change $\Delta n^{\rm pm}$ of the birefringence in uniaxial and lower-symmetry crystals. It follows from (1.5.7.18) that this birefringence is bilinear in the applied field. Bilinear magnetic birefringence can be observed in uniaxial crystals if the magnetic field is applied along the x axis perpendicular to the principal z axis. In the simplest case, a difference in the refractive indices n_x and n_y arises:

$$\Delta n^{\rm pm} = n_x - n_y = \frac{1}{2n_0}(\delta\varepsilon_{xx} - \delta\varepsilon_{yy}) = \frac{1}{2n_0}(\Gamma_{xxxx} - \Gamma_{yyxx}) H_x^2, \quad (1.5.7.19)$$

where n_0 is the refractive index for the ordinary beam.

Consider now a magnetically ordered crystal which can be characterized by an antiferromagnetic vector $\mathbf{L}_0$ and a magnetization vector $\mathbf{M}_0$ in the absence of a magnetic field. Applying a magnetic field with components H_r, we change the direction and size of $\mathbf{L}_0$ and $\mathbf{M}_0$, getting additional components $L^H_k = \chi^L_{kr} H_r$ and $M^H_k = \chi^M_{kr} H_r$. This is illustrated by the relations (1.5.7.6). Instead of (1.5.7.18) we get

$$\begin{aligned}\delta\varepsilon_{ij} &= Q^{LL}_{ijk\ell} L_k L_\ell + Q^{ML}_{ijk\ell} M_k L_\ell + Q^{MM}_{ijk\ell} M_k M_\ell \\ &= Q^{LL}_{ijk\ell} L_{0k} L_{0\ell} + Q^{ML}_{ijk\ell} M_{0k} L_{0\ell} + Q^{MM}_{ijk\ell} M_{0k} M_{0\ell} \\ &\quad + [2Q^{LL}_{ijk\ell} \chi^L_{kr} L_{0\ell} + Q^{ML}_{ijk\ell} (\chi^M_{kr} L_{0\ell} + M_{0k} \chi^L_{\ell r}) + 2Q^{MM}_{ijk\ell} \chi^M_{kr} M_{0\ell}] H_r. \end{aligned} \quad (1.5.7.20)$$

The terms in the middle line of (1.5.7.20) show that in an ordered state a change in the refractive indices occurs that is proportional to L_0^2 in antiferromagnets and to M_0^2 in ferromagnets. The terms in square brackets show that a linear magnetic birefringence may exist. In the special case of a tetragonal antiferromagnet belonging to the space group $\boldsymbol{D}^{14}_{4h} = P4_2/mnm$ with $\mathbf{L}_0$ parallel to the principal axis z, the linear birefringence occurs in the xy plane if the magnetic field is applied along the z axis (see Fig. 1.5.5.3). In this case, $\mathbf{M}_0 = 0$, $\chi^L_{kz} = 0$ for all k, $\chi^M_{xz} = \chi^M_{yz} = 0$ and $\chi^M_{zz} = 1/B$ [see (1.5.7.6)]. Therefore the terms in square brackets in (1.5.7.20) differ from zero only for one component of $\delta\varepsilon_{ij}$,

$$\delta\varepsilon_{ij} = Q^{ML}_{xyzz} L_{0z} H_z / B = q_{zxy} H_z \,\mathrm{sign}(L_{0z}). \quad (1.5.7.21)$$

As a result,

$$\Delta n^{\rm af} = n_{x'} - n_{y'} = \frac{1}{2n_0}\delta\varepsilon_{xy} = \frac{1}{2n_0} q_{zxy} H_z \,\mathrm{sign}(L_{0z}), \quad (1.5.7.22)$$

where x', y' are the optic axes, which in these tetragonal crystals are rotated by $\pi/4$ relative to the crystallographic axes.

Comparing relation (1.5.7.22) with (1.5.7.3), one can see that like LM, there may be linear magnetic birefringence. The forms of the tensors that describe the two effects are the same.

Linear magnetic birefringence has been observed in the uniaxial antiferromagnetic low-temperature α-Fe_2O_3 when the magnetic field was applied perpendicular to the threefold axis

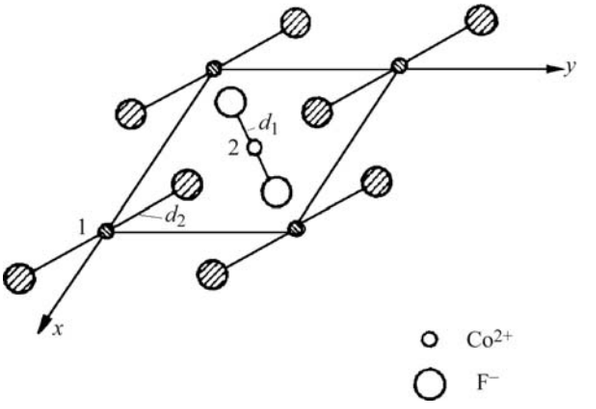

Fig. 1.5.7.3. Variation of symmetry of the crystal field in the presence of the piezomagnetic effect in CoF_2. The unshaded atoms lie at height $c/2$ above the xy plane (see Fig. 1.5.5.3).

(Le Gall *et al.*, 1977; Merkulov *et al.*, 1981). The most impressive effect was observed in CoF_2 when the magnetic field was applied along the fourfold axis. The crystal ceased to be optically uniaxial and a difference $(n_{x'} - n_{y'}) \propto H_z$ was observed in accordance with (1.5.7.22). Such linear magnetic birefringence does not exist in the paramagnetic state. Linear birefringence has also been observed in $CoCO_3$ and $DyFeO_3$. For details of these experiments, see Eremenko *et al.* (1989). These authors also used linear birefringence to make the antiferromagnetic domains visible. A further review of linear magnetic birefringence has been given by Ferré & Gehring (1984).

Piezomagnetism, linear magnetostriction and linear birefringence in fluorides can be clearly demonstrated qualitatively for one particular geometry. As shown in Fig. 1.5.7.3, the crystallographically equivalent points 1 and 2 are no longer equivalent after a shear deformation applied in the plane xy. During such a deformation, the distances from the magnetic ions to the nearest fluoride ions increase in points 1 and decrease in points 2. As a result, the values of the g-factors for the ions change. Evidently, the changes of the values of the g-factors for different sublattices are opposite in sign. Thus the sublattice magnetizations are no longer equal, and a magnetic moment arises along the direction of sublattice magnetization. On the other hand, if we increase the magnetization of one sublattice and decrease the magnetization of the other by applying a magnetic field parallel to the z axis, the interactions with the neighbouring fluoride ions also undergo changes with opposite signs. This gives rise to the magnetostriction. These considerations can be applied only to antiferromagnets with the fluoride structure. In these structures, single-ion anisotropy is responsible for the weak ferromagnetism, not the antisymmetric exchange interaction of the form $\mathbf{d}[\mathbf{S}_i \times \mathbf{S}_k]$.

1.5.8. Magnetoelectric effect

Curie (1894) stated that materials that develop an electric polarization in a magnetic field or a magnetization in an electric field may exist. This prediction was given a more precise form by Landau & Lifshitz (1957), who considered the invariants in the expansion of the thermodynamic potential up to linear terms in H_i. For materials belonging to certain magnetic point groups, the thermodynamic potential Φ can be written in the form

$$\Phi = \Phi_0 - \alpha_{ij} E_i H_j. \quad (1.5.8.1)$$

If (in the absence of a magnetic field) an electric field $\mathbf{E}$ is applied to a crystal with potential (1.5.8.1), a magnetization will be produced:

$$M_j = -\frac{\partial\Phi}{\partial H_j} = \alpha_{ij} E_i. \quad (1.5.8.2)$$

Conversely, an electric polarization **P** arises at zero electric field if a magnetic field is applied:

$$P_i = -\frac{\partial \Phi}{\partial E_i} = \alpha_{ij} H_j. \qquad (1.5.8.3)$$

This phenomenon is called the magnetoelectric effect. A distinction is made between the linear magnetoelectric effect described above and two types of bilinear magnetoelectric effects. These bilinear effects arise if the thermodynamic potential contains terms of the form $E_i H_j H_k$ or $H_i E_j E_k$. They will be described in Section 1.5.8.2.

1.5.8.1. *Linear magnetoelectric effect*

It is obvious that the linear magnetoelectric effect is forbidden for all dia- and paramagnets as their magnetic groups possess R as a separate element. The effect is also forbidden if the magnetic space group contains translations multiplied by R because in these cases the point group also possesses R as a separate element. Since **H** is an axial vector that changes sign under R and **E** is a polar vector that is invariant under time inversion, α_{ij} is an axial tensor of second rank, the components of which all change sign under time inversion (R). From relation (1.5.8.1), it follows that a magnetic group which allows the magnetoelectric effect cannot possess a centre of symmetry ($C_i = \bar{1}$). However, it can possess it multiplied by R ($C_i R = \bar{1}'$) (see Table 1.5.8.1). There are 21 magnetic point groups that possess a centre of symmetry. The detailed analysis of the properties of the tensor α_{ij} shows that among the remaining 69 point groups there are 11 groups for which the linear magnetoelectric effect is also forbidden. These groups are $\boldsymbol{C}_{3h} = \bar{6}$, $\boldsymbol{C}_6(\boldsymbol{C}_3) = 6'$, $\boldsymbol{C}_{6h}(\boldsymbol{C}_{3h}) = 6'/m$, $\boldsymbol{D}_{3h} = \bar{6}m2$, $\boldsymbol{D}_{3h}(\boldsymbol{C}_{3h}) = \bar{6}m'2'$, $\boldsymbol{D}_{6h}(\boldsymbol{D}_{3h}) = 6'/mmm'$, $\boldsymbol{D}_6(\boldsymbol{D}_3) = 6'22'$, $\boldsymbol{C}_{6v}(\boldsymbol{C}_{3v}) = 6'm'm$, $\boldsymbol{T}_d = \bar{4}3m$, $\boldsymbol{O}(\boldsymbol{T}) = 4'32'$ and $\boldsymbol{O}_h(\boldsymbol{T}_d) = m'\bar{3}'m$.

All remaining 58 magnetic point groups in which the linear magnetoelectric effect is possible are listed in Table 1.5.8.1. The 11 forms of tensors that describe this effect are also listed in this table.[3] The orientation of the axes of the Cartesian coordinate system (CCS) with respect to the symmetry axes of the crystal is the same as in Table 1.5.7.1. Alternative orientations of the same point group that give rise to the same form of α_{ij} have been added between square brackets in Table 1.5.8.1. The tensor has the same form for 32 (= 321) and 312, $3m'1$ and $31m'$, $\bar{3}'m'1$ and $\bar{3}'1m'$; it also has the same form for $3m1$ and $31m$, $32'1$ and $312'$, $\bar{3}'m1$ and $\bar{3}'1m$.

The forms of α_{ij} for frequently encountered orientations of the CCS other than those given in Table 1.5.8.1 are (*cf.* Rivera, 1994)

(1) $112, 11m', 11\,2/m'$ (unique axis z):

$$\begin{bmatrix} \alpha_{11} & \alpha_{12} & 0 \\ \alpha_{21} & \alpha_{22} & 0 \\ 0 & 0 & \alpha_{33} \end{bmatrix};$$

(2) $11m, 112', 11\,2'/m$ (unique axis z):

$$\begin{bmatrix} 0 & 0 & \alpha_{13} \\ 0 & 0 & \alpha_{23} \\ \alpha_{31} & \alpha_{32} & 0 \end{bmatrix};$$

(3) $2mm, 22'2', m'm2'\,[m'2'm], m'mm$:

$$\begin{bmatrix} 0 & 0 & 0 \\ 0 & 0 & \alpha_{23} \\ 0 & \alpha_{32} & 0 \end{bmatrix};$$

(4) $m2m, 2'22', mm'2'\,[2'm'm], mm'm$:

$$\begin{bmatrix} 0 & 0 & \alpha_{13} \\ 0 & 0 & 0 \\ \alpha_{31} & 0 & 0 \end{bmatrix};$$

(5) $\bar{4}m2, \bar{4}2'm', 4'2'2, 4'mm', 4'/m'mm'$:

$$\begin{bmatrix} 0 & \alpha_{12} & 0 \\ \alpha_{12} & 0 & 0 \\ 0 & 0 & 0 \end{bmatrix}.$$

Table 1.5.8.1. *The forms of the tensor characterizing the linear magnetoelectric effect*

Magnetic crystal class		Matrix representation of the property tensor α_{ij}
Schoenflies	Hermann–Mauguin	
$\boldsymbol{C}_1$ $\boldsymbol{C}_i(\boldsymbol{C}_1)$	1 $\bar{1}'$	$\begin{bmatrix} \alpha_{11} & \alpha_{12} & \alpha_{13} \\ \alpha_{21} & \alpha_{22} & \alpha_{23} \\ \alpha_{31} & \alpha_{32} & \alpha_{33} \end{bmatrix}$
$\boldsymbol{C}_2$ $\boldsymbol{C}_s(\boldsymbol{C}_1)$ $\boldsymbol{C}_{2h}(\boldsymbol{C}_2)$	$2\,(=121)$ $m'\,(=1m'1)$ $2/m'\,(=1\,2/m'\,1)$ (unique axis y)	$\begin{bmatrix} \alpha_{11} & 0 & \alpha_{13} \\ 0 & \alpha_{22} & 0 \\ \alpha_{31} & 0 & \alpha_{33} \end{bmatrix}$
$\boldsymbol{C}_s$ $\boldsymbol{C}_2(\boldsymbol{C}_1)$ $\boldsymbol{C}_{2h}(\boldsymbol{C}_s)$	$m\,(=1m1)$ $2'\,(=12'1)$ $2'/m\,(=1\,2'/m\,1)$ (unique axis y)	$\begin{bmatrix} 0 & \alpha_{12} & 0 \\ \alpha_{21} & 0 & \alpha_{23} \\ 0 & \alpha_{32} & 0 \end{bmatrix}$
$\boldsymbol{D}_2$ $\boldsymbol{C}_{2v}(\boldsymbol{C}_2)$ $\boldsymbol{D}_{2h}(\boldsymbol{D}_2)$	222 $m'm'2\,[2m'm',\ m'2m']$ $m'm'm'$	$\begin{bmatrix} \alpha_{11} & 0 & 0 \\ 0 & \alpha_{22} & 0 \\ 0 & 0 & \alpha_{33} \end{bmatrix}$
$\boldsymbol{C}_{2v}$ $\boldsymbol{D}_2(\boldsymbol{C}_2)$ $\boldsymbol{C}_{2v}(\boldsymbol{C}_s)$ $\boldsymbol{D}_{2h}(\boldsymbol{C}_{2v})$	$mm2$ $2'2'2$ $2'mm'\,[m2'm']$ mmm'	$\begin{bmatrix} 0 & \alpha_{12} & 0 \\ \alpha_{21} & 0 & 0 \\ 0 & 0 & 0 \end{bmatrix}$
$\boldsymbol{C}_4,\ \boldsymbol{S}_4(\boldsymbol{C}_2),\ \boldsymbol{C}_{4h}(\boldsymbol{C}_4)$ $\boldsymbol{C}_3,\ \boldsymbol{S}_6(\boldsymbol{C}_3)$ $\boldsymbol{C}_6,\ \boldsymbol{C}_{3h}(\boldsymbol{C}_3),\ \boldsymbol{C}_{6h}(\boldsymbol{C}_6)$	$4,\ \bar{4}',\ 4/m'$ $3,\ \bar{3}'$ $6,\ \bar{6}',\ 6/m'$	$\begin{bmatrix} \alpha_{11} & \alpha_{12} & 0 \\ -\alpha_{12} & \alpha_{11} & 0 \\ 0 & 0 & \alpha_{33} \end{bmatrix}$
$\boldsymbol{S}_4$ $\boldsymbol{C}_4(\boldsymbol{C}_2)$ $\boldsymbol{C}_{4h}(\boldsymbol{S}_4)$	$\bar{4}$ $4'$ $4'/m'$	$\begin{bmatrix} \alpha_{11} & \alpha_{12} & 0 \\ \alpha_{12} & -\alpha_{11} & 0 \\ 0 & 0 & 0 \end{bmatrix}$
$\boldsymbol{D}_4,\ \boldsymbol{C}_{4v}(\boldsymbol{C}_4)$ $\boldsymbol{D}_{2d}(\boldsymbol{D}_2),\ \boldsymbol{D}_{4h}(\boldsymbol{D}_4)$ $\boldsymbol{D}_3,\ \boldsymbol{C}_{3v}(\boldsymbol{C}_3),\ \boldsymbol{D}_{3d}(\boldsymbol{D}_3)$ $\boldsymbol{D}_6,\ \boldsymbol{C}_{6v}(\boldsymbol{C}_6)$ $\boldsymbol{D}_{3h}(\boldsymbol{D}_3),\ \boldsymbol{D}_{6h}(\boldsymbol{D}_6)$	$422,\ 4m'm'$ $\bar{4}'2m'\,[\bar{4}'m'2],\ 4/m'm'm'$ $32,\ 3m',\ \bar{3}'m'$ $622,\ 6m'm'$ $\bar{6}'m'2\,[\bar{6}'2m'],\ 6/m'm'm'$	$\begin{bmatrix} \alpha_{11} & 0 & 0 \\ 0 & \alpha_{11} & 0 \\ 0 & 0 & \alpha_{33} \end{bmatrix}$
$\boldsymbol{C}_{4v},\ \boldsymbol{D}_4(\boldsymbol{C}_4)$ $\boldsymbol{D}_{2d}(\boldsymbol{C}_{2v}),\ \boldsymbol{D}_{4h}(\boldsymbol{C}_{4v})$ $\boldsymbol{C}_{3v},\ \boldsymbol{D}_3(\boldsymbol{C}_3),\ \boldsymbol{D}_{3d}(\boldsymbol{C}_{3v})$ $\boldsymbol{C}_{6v},\ \boldsymbol{D}_6(\boldsymbol{C}_6)$ $\boldsymbol{D}_{3h}(\boldsymbol{C}_{3v}),\ \boldsymbol{D}_{6h}(\boldsymbol{D}_{6v})$	$4mm,\ 42'2'$ $\bar{4}'2'm\,[\bar{4}'m2'],\ 4/m'mm$ $3m,\ 32',\ \bar{3}'m$ $6mm,\ 62'2'$ $\bar{6}'m2'\,[\bar{6}'2'm],\ 6/m'mm$	$\begin{bmatrix} 0 & \alpha_{12} & 0 \\ -\alpha_{12} & 0 & 0 \\ 0 & 0 & 0 \end{bmatrix}$
$\boldsymbol{D}_{2d},\ \boldsymbol{D}_{2d}(\boldsymbol{S}_4)$ $\boldsymbol{D}_4(\boldsymbol{D}_2),\ \boldsymbol{C}_{4v}(\boldsymbol{C}_{2v})$ $\boldsymbol{D}_{4h}(\boldsymbol{D}_{2d})$	$\bar{4}2m,\ \bar{4}m'2'$ $4'22',\ 4'm'm$ $4'/m'm'm$	$\begin{bmatrix} \alpha_{11} & 0 & 0 \\ 0 & -\alpha_{11} & 0 \\ 0 & 0 & 0 \end{bmatrix}$
$\boldsymbol{T},\ \boldsymbol{T}_h(\boldsymbol{T})$ $\boldsymbol{O},\ \boldsymbol{T}_d(\boldsymbol{T}),\ \boldsymbol{O}_h(\boldsymbol{O})$	$23,\ m'\bar{3}'$ $432,\ \bar{4}'3m',\ m'\bar{3}'m'$	$\begin{bmatrix} \alpha_{11} & 0 & 0 \\ 0 & \alpha_{11} & 0 \\ 0 & 0 & \alpha_{11} \end{bmatrix}$

[3] Table 1.5.8.1 shows that the tensor describing the magnetoelectric effect does not need to be symmetric for 31 of the 58 point groups. These 31 groups coincide with those that admit a spontaneous toroidal moment (Gorbatsevich & Kopaev, 1994); they were first determined by Ascher (1966) as the magnetic point groups admitting spontaneous currents.

As mentioned above, the components of the linear magnetoelectric tensor change sign under time inversion. The sign of these components is defined by the sign of the antiferromagnetic vector **L**, *i.e.* by the sign of the 180° domains (S-domains). This is like the behaviour of the piezomagnetic effect and therefore everything said above about the role of the domains can be applied to the magnetoelectric effect.

Dzyaloshinskii (1959) proposed the antiferromagnetic Cr_2O_3 as the first candidate for the observation of the magnetoelectric (ME) effect. He showed that the ME tensor for this compound has three nonzero components: $\alpha_{11} = \alpha_{22}$ and α_{33}. The ME effect in Cr_2O_3 was discovered experimentally by Astrov (1960) on an unoriented crystal. He verified that the effect is linear in the applied electric field. Folen *et al.* (1961) and later Astrov (1961) performed measurements on oriented crystals and revealed the anisotropy of the ME effect. In the first experiments, the ordinary magnetoelectric effect ME_E (the electrically induced magnetization) was investigated. This means the magnetic moment induced by the applied electric field was measured. Later Rado & Folen (1961) observed the converse effect ME_H (the electric polarization induced by the magnetic field). The temperature dependence of the components of the magnetoelectric tensor in Cr_2O_3 was studied in detail in both laboratories.

In the following years, many compounds that display the linear magnetoelectric effect were discovered. Both the electrically induced and the magnetically induced ME effect were observed. The values of the components of the magnetoelectric tensor range from 10^{-6} to 10^{-2} in compounds containing the ions of the iron group and from 10^{-4} to 10^{-2} in rare-earth compounds. Cox (1974) collected values of α_{max} of the known magnetoelectrics. Some are listed in Table 1.5.8.2 together with more recent results.

Table 1.5.8.2. *A list of some magnetoelectrics*

Compound	T_N or T_C (K)	Magnetic point group	Maximum α_{obs}	References†
Fe_2TeO_6	219	$4/m'm'm'$	3×10^{-5}	7–9, 70
$DyAlO_3$	3.5	$m'm'm'$	2×10^{-3}	11–13
$GdAlO_3$	4.0	$m'm'm'$	1×10^{-4}	14
$TbAlO_3$	4.0	$m'm'm'$	1×10^{-3}	12, 15–17
$TbCoO_3$	3.3	mmm'	3×10^{-5}	12, 16, 18
Cr_2O_3	318	$\bar{3}'m'$	1×10^{-4}	45–49, 70, 71, W162
$Nb_2Mn_4O_9$	110	$\bar{3}'m'$	2×10^{-6}	52, 53
$Nb_2Co_4O_9$	27	$\bar{3}'m'$	2×10^{-5}	52, 53
$Ta_2Mn_4O_9$	104	$\bar{3}'m'$	1×10^{-5}	53
$Ta_2Co_4O_9$	21	$\bar{3}'m'$	1×10^{-4}	53
$LiMnPO_4$	35	$m'm'm'$	2×10^{-5}	55, 56, 58, 60
$LiFePO_4$	50	mmm'	1×10^{-4}	57, 58
$LiCoPO_4$	22	mmm'	7×10^{-4}	54, 55, R161
$LiNiPO_4$	23	mmm'	4×10^{-5}	54, 55, 61
$GdVO_4$	2.4	$4'/m'm'm$	3×10^{-4}	70
$TbPO_4$	2.2	$4'/m'm'm$	1×10^{-2}	66, 67
$DyPO_4$	3.4	$4'/m'm'm$	1×10^{-3}	68, 69
$HoPO_4$	1.4	$4'/m'm'm$	2×10^{-4}	72
$Mn_3B_7O_{13}I$	26	$m'm2'$	2×10^{-6}	C204
$Co_3B_7O_{13}Cl$	12	m	3×10^{-4}	S204
$Co_3B_7O_{13}Br$	17	$m'm2'$	2×10^{-3}	88C1
$Co_3B_7O_{13}I$	38	$m'm2'$	1×10^{-3}	90C3
$Ni_3B_7O_{13}I$	61.5	m'	2×10^{-4}	74, 75, 77–79, 90C2
$Ni_3B_7O_{13}Cl$	9	$m'm2'$	3×10^{-4}	74R2, 91R1
$Cu_3B_7O_{13}Cl$	8.4	$m'm'2$	3×10^{-6}	88R1
$FeGaO_3$	305	$m'm2'$	4×10^{-4}	84–86
TbOOH	10.0	$2/m'$	4×10^{-4}	114
DyOOH	7.2	$2/m'$	1×10^{-4}	92, 114
ErOOH	4.1	$2'/m$	5×10^{-4}	93, 114
Gd_2CuO_4	6.5	mmm'	1×10^{-4}	W161
$MnNb_2O_6$	4.4	mmm'	3×10^{-6}	101, 102
$MnGeO_3$	16	mmm'	2×10^{-6}	98–100
$CoGeO_3$	31	mmm'	1×10^{-4}	70
$CrTiNdO_5$	13	mmm'	1×10^{-5}	70, 89

† Numbers refer to references quoted by Cox (1974); codes 88C1, 90C3, 88R1, 90C2, 74R2, 91R1 refer to references quoted by Burzo (1993); and codes W162, R161, C204, S204 and W161 refer to articles in *Ferroelectrics*, **162**, 141, **161**, 147, **204**, 125, **204**, 57 and **161**, 133, respectively.

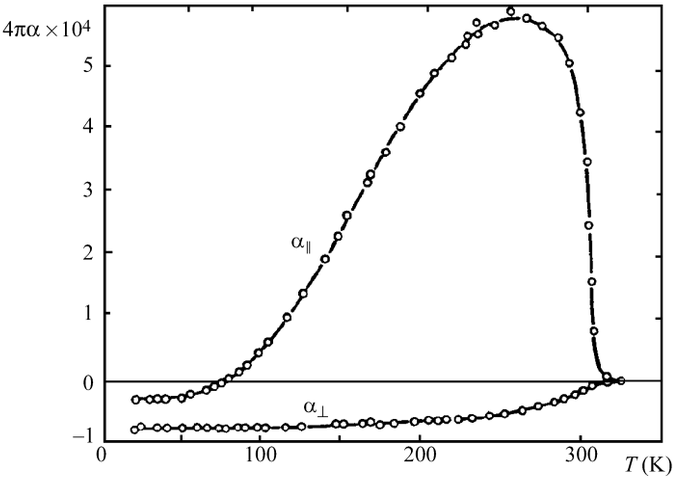

Fig. 1.5.8.1. Temperature dependence of the components $\alpha_\parallel$ and $\alpha_\perp$ in Cr_2O_3 (Astrov, 1961).

Additional information about the experimental data is presented in three conference proceedings (Freeman & Schmid, 1975; Schmid *et al.*, 1994; Bichurin, 1997).

The values of α_{ij} are given in rationalized Gaussian units, where α_{ij} is dimensionless. Some authors follow Dzyaloshinskii (1959) in writing (1.5.8.1) as $\Phi = \Phi_0 - (\alpha'_{ij}/4\pi)E_iH_j$, where α'_{ij} are the non-rationalized Gaussian values of the components of the magnetoelectric tensor. If SI units are used, then (1.5.8.1) becomes $\Phi = \Phi_0 - \alpha^{SI}_{ij}E_iH_j$. The connections between the values of a tensor component expressed in these three systems are

$$4\pi\alpha_{ij} = \alpha'_{ij} = 3 \times 10^8 \alpha^{SI}_{ij}. \qquad (1.5.8.4)$$

The units of α^{SI}_{ij} are s m^{-1}. A detailed discussion of the relations between the descriptions of the magnetoelectric effect in different systems of units is given by Rivera (1994).

Most magnetoelectrics are oxides containing magnetic ions. The ions of the iron group are contained in corundum-type oxides [magnetic point group $\boldsymbol{D}_{3d}(\boldsymbol{D}_3) = \bar{3}'m'$], triphyllite-type oxides with different magnetic groups belonging to the orthorhombic crystallographic structure $\boldsymbol{D}_{2h} = mmm$ and other compounds. The rare-earth oxides are represented by the orthorhombic RMO_3 structure with R = rare earth, $M = Fe^{3+}$, Co^{3+}, Al^{3+} [magnetic point group $\boldsymbol{D}_{2h}(\boldsymbol{D}_2) = m'm'm'$], tetragonal zircon-type compounds RMO_4 (R = rare earth, M = P, V) [magnetic point group $\boldsymbol{D}_{4h}(\boldsymbol{D}_{2d}) = 4'/m'm'm$], monoclinic oxide hydroxides ROOH [magnetic point groups $\boldsymbol{C}_{2h}(\boldsymbol{C}_2) = 2/m'$, $\boldsymbol{C}_{2h}(\boldsymbol{C}_s) = 2'/m$] and other compounds. Of particular interest is $TbPO_4$, which has the highest value of the magnetoelectric tensor components, 1.2×10^{-2} (Rado & Ferrari, 1973; Rado *et al.*, 1984). There are also some weak ferromagnets and ferrimagnets that exhibit the linear magnetoelectric effect. An example is the weakly ferromagnetic boracite $Ni_3B_7O_{13}I$. These orthorhombic compounds will be discussed in Section 1.5.8.3. Another orthorhombic magnetoelectric crystal is ferrimagnetic $FeGaO_3$ (Rado, 1964; see Table 1.5.8.2).

It has been shown in experiments on Cr_2O_3 that in the spin-flop phase $\alpha_\parallel$ becomes zero but a non-diagonal component α_{xz} arises (Popov *et al.*, 1992). Such behaviour is possible if under the spin-flop transition the magnetic point group of Cr_2O_3 transforms from $\boldsymbol{D}_{3d}(\boldsymbol{D}_3) = \bar{3}'m'$ to $\boldsymbol{C}_{2h}(\boldsymbol{C}_s) = 112'/m$. For the latter magnetic point group, the ME tensor possesses only transverse components.

The temperature dependences determined for the ME moduli, $\alpha_\parallel$ and $\alpha_\perp$, in Cr_2O_3 are quite different (see Fig. 1.5.8.1). The temperature dependence of $\alpha_\perp$ is similar to that of the order parameter (sublattice magnetization M_0), which can be explained easily, bearing in mind that the magnetoelectric moduli are

proportional to the magnitude of the antiferromagnetic vector ($\alpha \propto L_z = 2M_0$). However, to explain the rather complicated temperature dependence of $\alpha_\parallel$ it becomes necessary to assume that the moduli α are proportional to the magnetic susceptibility of the crystal so that (Rado, 1961; Rado & Folen, 1962)

$$\alpha_\parallel = a_\parallel \chi_\parallel L_z, \quad \alpha_\perp = a_\perp \chi_\perp L_z, \tag{1.5.8.5}$$

where $a_\parallel$ and $a_\perp$ are new constants of the magnetoelectric effect which do not depend on temperature. Formulas (1.5.8.5) provide a good explanation of the observed temperature dependence of α.

The linear relation between α and $L_z = 2M_0$ is also proved by the fact that when studying the ME effect, the domain structure of the sample is revealed. An annealing procedure to prepare a single-domain sample has been developed. To perform this annealing, the sample must be heated well above the Néel temperature and then cooled below T_N in the presence of electric and magnetic fields. The directions of these fields have to agree with the allowed components of the ME tensor. In some compounds, a single-domain state may be obtained by applying simultaneous pulses of both fields to a multidomain sample at temperatures below T_N (see O'Dell, 1970).

It was shown in the previous section that the piezomagnetic effect can be explained phenomenologically as weak ferromagnetism caused by the change of the symmetry produced by deformation of the lattice. The electric field may act indirectly inducing atomic displacement (similar to the displacement under stress) and as in piezomagnetism may cause the rise of a magnetic moment. Such ideas were proposed by Rado (1964) and expanded by White (1974).

The electric field may act directly to change the admixture of orbital states in the electron wavefunctions. As a result of such direct action, there may be a change of different terms in the microscopic spin Hamiltonian. Correspondingly, the following mechanisms are to be distinguished. Changes in the g-tensor can explain the ME effect in $DyPO_4$ (Rado, 1969). The electric-field-induced changes in single-ion anisotropy may represent the main mechanism of the ME effect in Cr_2O_3 (Rado, 1962). Two other mechanisms have to be taken into account: changes in symmetric and antisymmetric exchange. For details and references see the review article of de Alcantara Bonfim & Gehring (1980).

1.5.8.2. *Nonlinear magnetoelectric effects*

Along with linear terms in E and H, the thermodynamic potential Φ may also contain invariants of higher order in E_k, H_i:

$$\Phi = \Phi_0 - \alpha_{ik}E_iH_k - \tfrac{1}{2}\beta_{ijk}E_iH_jH_k - \tfrac{1}{2}\gamma_{ijk}H_iE_jE_k. \tag{1.5.8.6}$$

From this relation, one obtains the following formulas for the electric polarization P_i and the magnetization M_i:

$$P_i = \alpha_{ik}H_k + \tfrac{1}{2}\beta_{ijk}H_jH_k + \gamma_{jik}H_jE_k, \tag{1.5.8.7}$$

$$M_i = \alpha_{ki}E_k + \beta_{jik}E_jH_k + \tfrac{1}{2}\gamma_{ijk}E_jE_k. \tag{1.5.8.8}$$

The third term in (1.5.8.7) describes the dependence of the dielectric susceptibility ($\chi^e_{ik} = P_i/E_k$) and, consequently, of the dielectric permittivity ε_{ik}, on the magnetic field. Similarly, the second term in (1.5.8.8) points out that the magnetic susceptibility χ^m may depend on the electric field ($\delta\chi^m_{ik} = \beta_{jik}E_j$). The tensors β_{ijk} and γ_{ijk} are symmetric in their last two indices. Symmetry imposes on β_{ijk} the same restrictions as on the piezoelectric tensor and on γ_{ijk} the same restrictions as on the piezomagnetic tensor (see Table 1.5.7.1).

Ascher (1968) determined all the magnetic point groups that allow the terms EHH and HEE in the expansion of the thermodynamic potential Φ. These groups are given in Table 1.5.8.3, which has been adapted from a table given by Schmid (1973). It classifies the 122 magnetic point groups according to which types of magnetoelectric effects (EH, EHH or HEE) they admit and whether they admit spontaneous dielectric polarization (E) or spontaneous magnetization (H). It also classifies the 122 point groups according to whether they contain $\bar{1}$, $1'$ or $\bar{1}'$, as in a table given by Mercier (1974). Ferromagnets, ferrimagnets and weak ferromagnets have a point group characterized by H (the 31 groups of types 4–7 in Table 1.5.8.3); dia- and paramagnets as well as antiferromagnets with a nontrivial magnetic Bravais lattice have a point group containing $1'$ (the 32 groups of types 1, 13, 17 and 19 in Table 1.5.8.3). The 59 remaining point groups describe antiferromagnets with a trivial Bravais lattice. The 31 point groups characterized by E, the 32 containing $\bar{1}$ and the 59 remaining ones correspond to a similar classification of crystals according to their electric properties (see Schmid, 1973).

Table 1.5.8.3 shows that for the 16 magnetic point groups of types 16–19, any kind of magnetoelectric effect is prohibited.

Table 1.5.8.3. *Classification of the 122 magnetic point groups according to magnetoelectric types*

Type	Inversions in the group	Permitted terms in thermodynamic potential	Magnetic point groups	Number of magnetic point groups				
1	$1'$	E EHH	$1'$, $21'$, $m1'$, $mm21'$, $41'$, $4mm1'$, $31'$, $3m1'$, $61'$, $6mm1'$	10	31		49	122
2		E EHH HEE	$6'$, $6'mm'$	2				
3		E EH EHH HEE	$mm2$, $4mm$, $4'$, $4'mm'$, $3m$, $6mm$	6				
4		E H EH EHH HEE	1, 2, m, $2'$, m', $m'm2'$, $m'm'2$, 4, $4m'm'$, 3, $3m'$, 6, $6m'm'$	13		31		
5		H EH EHH HEE	$2'2'2$, $42'2'$, $\bar{4}$, $\bar{4}2'm'$, $32'$, $62'2'$	6				
6		H EHH HEE	$\bar{6}$, $\bar{6}m'2'$	2				
7	$\bar{1}$	H HEE	$\bar{1}$, $2/m$, $2'/m'$, $m'm'm$, $4/m$, $4/mm'm'$, $\bar{3}$, $\bar{3}m'$, $6/m$, $6/mm'm'$	10				
8		EH EHH HEE	222, $\bar{4}'$, 422, $\bar{4}2m$, $4'22'$, $\bar{4}'2m'$, $\bar{4}'2'm$, 32, $\bar{6}'$, 622, $\bar{6}'m'2$, $\bar{6}'m2'$, 23, $\bar{4}'3m'$	14			73	
9		EHH HEE	$\bar{6}m2$, $6'22'$	2				
10		EH	432	1		19		
11	$\bar{1}'$	EH	$\bar{1}'$, $2/m'$, $2'/m$, mmm', $m'm'm'$, $4/m'$, $4'/m'$, $4/m'm'm'$, $4/m'mm$, $4'/m'm'm$, $\bar{3}'$, $\bar{3}'m'$, $\bar{3}'m$, $6/m'$, $6/m'm'm'$, $6/m'mm$, $m'\bar{3}'$, $m'\bar{3}'m'$	18				
12		EHH	$\bar{4}3m$	1		11		
13	$1'$	EHH	$2221'$, $\bar{4}1'$, $4221'$, $\bar{4}2m1'$, $321'$, $\bar{6}1'$, $6221'$, $\bar{6}m21'$, $231'$, $\bar{4}3m1'$	10				
14		HEE	$4'32'$	1		11		
15	$\bar{1}$	HEE	mmm, $4'/m$, $4/mmm$, $4'/mmm'$, $\bar{3}m$, $6'/m'$, $6/mmm$, $6'/m'm'm$, $m\bar{3}$, $m\bar{3}m'$	10				
16	$\bar{1}'$		$6'/m$, $6'/mmm'$, $m'\bar{3}'m$	3		16		
17	$1'$		$4321'$	1				
18	$\bar{1}$		$m\bar{3}m$	1				
19	$\bar{1}$, $1'$, $\bar{1}'$		$\bar{1}1'$, $2/m1'$, $mmm1'$, $4/m1'$, $4/mmm1'$, $\bar{3}1'$, $\bar{3}m1'$, $6/m1'$, $6/mmm1'$, $m\bar{3}1'$, $m\bar{3}m1'$	11				

These are the 11 grey point groups that contain all three inversions, the white group $\boldsymbol{O}_h = m\bar{3}m$, the grey group $(\boldsymbol{O} + R\boldsymbol{O}) = 4321'$ and the three black–white groups $\boldsymbol{C}_{6h}(\boldsymbol{C}_{3h}) = 6'/m$, $\boldsymbol{D}_{6h}(\boldsymbol{D}_{3h}) = 6'/mmm'$ and $\boldsymbol{O}_h(\boldsymbol{T}_d) = m'\bar{3}'m$.

Among the 58 magnetic point groups that allow the linear magnetoelectric effect, there are 19 that do not allow the nonlinear effects EHH and HEE (types 10 and 11 in Table 1.5.8.3). The remaining 39 groups are compatible with all three effects, EH, EHH and HEE; 19 of these groups describe ferromagnets (including weak ferromagnets) and ferrimagnets (types 4 and 5 in Table 1.5.8.3).

The 21 point groups of types 7, 14 and 15 allow only the magnetoelectric effect *HEE*. These groups contain $\boldsymbol{C}_i = \bar{1}$, except $4'32'$. The compounds belonging to these groups possess only one tensor of magnetoelectric susceptibility, the tensor γ_{ijk} of the nonlinear ME effect. The effect is described by

$$P_i = \gamma_{jik} H_j E_k, \tag{1.5.8.9}$$

$$M_i = \tfrac{1}{2}\gamma_{ijk} E_j E_k. \tag{1.5.8.10}$$

The magnetic point group of ferrimagnetic rare-earth garnets $R\mathrm{Fe}_5\mathrm{O}_{12}$ (R = Gd, Y, Dy) is $\boldsymbol{D}_{3d}(\boldsymbol{S}_6) = \bar{3}m'$, which is of type 7. Therefore, the rare-earth garnets may show a nonlinear ME effect corresponding to relations (1.5.8.9) and (1.5.8.10). This was observed by O'Dell (1967) by means of a pulsed magnetic field. As mentioned above, this effect may be considered as the dependence of the dielectric permittivity on the magnetic field, which was the method used by Cardwell (1969) to investigate this ME effect experimentally. Later Lee *et al.* (1970) observed the ME effect defined by relation (1.5.8.10). Applying both static electric fields and alternating ones (at a frequency ω), they observed an alternating magnetization at both frequencies ω and 2ω. A nonlinear ME effect of the form *HEE* was also observed in the weakly ferromagnetic orthoferrites TbFeO_3 and YbFeO_3. Their magnetic point group is $\boldsymbol{D}_{2h}(\boldsymbol{C}_{2h}) = m'm'm$.

Moreover, paramagnets that do not possess an inversion centre $\boldsymbol{C}_i = \bar{1}$ may show an ME effect if the point group is not $4321'$. They have one of the 20 grey point groups given as types 1 or 13 in Table 1.5.8.3. Bloembergen (1962) pointed out that all these paramagnets are piezoelectric crystals. He called the ME effect in these substances the *paramagnetoelectric* (PME) effect. It is defined by the nonzero components of the tensor β_{ijk}:

$$P_i = \tfrac{1}{2}\beta_{ijk} H_j H_k, \tag{1.5.8.11}$$

$$M_i = \beta_{jik} E_j H_k. \tag{1.5.8.12}$$

The PME effect was discovered by Hou & Bloembergen (1965) in $\mathrm{NiSO}_4{\cdot}6\mathrm{H}_2\mathrm{O}$, which belongs to the crystallographic point group $\boldsymbol{D}_4 = 422$. The only nonvanishing components of the third-rank tensor are $\beta_{xyz} = \beta_{xzy} = -\beta_{yzx} = -\beta_{yxz} = \beta$ ($\beta_{14} = -\beta_{25} = 2\beta$ in matrix notation), so that $\mathbf{P} = \beta(H_y H_z, -H_x H_z, 0)$ and $\mathbf{M} = \beta(-E_y H_z,\ E_x H_z,\ E_x H_y - E_y H_x)$. Both effects were observed: the polarization $\mathbf{P}$ by applying static (H_z) and alternating (H_x or H_y) magnetic fields and the magnetization $\mathbf{M}$ by applying a static magnetic field H_z and an alternating electric field in the plane xy. As a function of temperature, the PME effect shows a peak at 3.0 K and changes sign at 1.38 K. The coefficient of the PME effect at 4.2 K is

$$\beta(4.2\ \mathrm{K}) = 2.2 \times 10^{-9}\ \text{cgs units}. \tag{1.5.8.13}$$

The theory developed by Hou and Bloembergen explains the PME effect by linear variation with the applied electric field of the crystal-field-splitting parameter D of the spin Hamiltonian.

Most white and black–white magnetic point groups that do not contain the inversion ($\boldsymbol{C}_i = \bar{1}$), either by itself or multiplied by $R = 1'$, admit all three types of ME effect: the linear (*EH*) and two higher-order (*EHH* and *HEE*) effects. There are many magnetically ordered compounds in which the nonlinear ME effect has been observed. Some of them are listed by Schmid (1973); more recent references are given in Schmid (1994*a*).

In principle, many ME effects of higher order may exist. As an example, let us consider the *piezomagnetoelectric* effect. This is a combination of piezomagnetism (or piezoelectricity) and the ME effect. The thermodynamic potential Φ must contain invariants of the form

$$\Phi = \Phi_0 - \pi_{ijk\ell} E_i H_j T_{k\ell}. \tag{1.5.8.14}$$

The problem of the piezomagnetoelectric effect was considered by Rado (1962), Lyubimov (1965) and recently in detail by Grimmer (1992). All 69 white and black–white magnetic point groups that possess neither $\boldsymbol{C}_i = \bar{1}$ nor $R = 1'$ admit the piezomagnetoelectric effect. (These are the groups of types 2–6, 8–12, 14 and 16 in Table 1.5.8.3.) The tensor $\pi_{ijk\ell}$ that describes the piezomagnetoelectric effect is a tensor of rank 4, symmetric in the last two indices and invariant under space-time inversion. This effect has not been observed so far (Rivera & Schmid, 1994). Grimmer (1992) analyses in which antiferromagnets it could be observed.

1.5.8.3. *Ferromagnetic and antiferromagnetic ferroelectrics*

Neronova & Belov (1959) pointed out that there are ten magnetic point groups that admit the simultaneous existence of spontaneous dielectric polarization **P** and magnetic polarization **M**. Materials with such a complicated ordered structure are called ferromagnetoelectrics. Neronova and Belov considered only structures with parallel alignment of **P** and **M** (or **L**). There are three more groups that allow the coexistence of ferroelectric and ferromagnetic order, in which **P** and **M** are perpendicular to each other. Shuvalov & Belov (1962) published a list of the 13 magnetic point groups that admit ferromagnetoelectric order. These are the groups of type 4 in Table 1.5.8.3; they are given with more details in Table 1.5.8.4.

Notice that **P** and **M** must be parallel in eight point groups, they may be parallel in 1 and m', and they must be perpendicular in $2'$, m and $m'm2'$ (see also Ascher, 1970). The magnetic point groups listed in Table 1.5.8.4 admit not only ferromagnetism (and ferrimagnetism) but the first seven also admit antiferromagnetism with weak ferromagnetism. Ferroelectric pure antiferromagnets of type III^a may also exist. They must belong to one of the following eight magnetic point groups (types 2 and 3 in Table 1.5.8.3): $\boldsymbol{C}_4(\boldsymbol{C}_2) = 4'$; $\boldsymbol{C}_{4v}(\boldsymbol{C}_{2v}) = 4'mm'$; $\boldsymbol{C}_6(\boldsymbol{C}_3) = 6'$; $\boldsymbol{C}_{6v}(\boldsymbol{C}_{3v}) = 6'mm'$; $\boldsymbol{C}_{2v} = mm2$; $\boldsymbol{C}_{4v} = 4mm$; $\boldsymbol{C}_{3v} = 3m$; $\boldsymbol{C}_{6v} = 6mm$.

The first experimental evidence to indicate that complex perovskites may become ferromagnetoelectric was observed by the Smolenskii group (see Smolenskii *et al.*, 1958). They investigated the temperature dependence of the magnetic susceptibility of the ferroelectric perovskites $\mathrm{Pb(Mn_{1/2}Nb_{1/2})O_3}$ and $\mathrm{Pb(Fe_{1/2}Nb_{1/2})O_3}$. The temperature dependence at $T > 77$ K followed the Curie–Weiss law with a very large antiferromagnetic

Table 1.5.8.4. *List of the magnetic point groups of the ferromagnetoelectrics*

Symbol of symmetry group		Allowed direction of	
Schoenflies	Hermann–Mauguin	**P**	**M**
$\boldsymbol{C}_1$	1	Any	Any
$\boldsymbol{C}_2$	2	$\parallel 2$	$\parallel 2$
$\boldsymbol{C}_2(\boldsymbol{C}_1)$	$2'$	$\parallel 2'$	$\perp 2'$
$\boldsymbol{C}_s = \boldsymbol{C}_{1h}$	m	$\parallel m$	$\perp m$
$\boldsymbol{C}_s(\boldsymbol{C}_1)$	m'	$\parallel m'$	$\parallel m'$
$\boldsymbol{C}_{2v}(\boldsymbol{C}_2)$	$m'm'2$	$\parallel 2$	$\parallel 2$
$\boldsymbol{C}_{2v}(\boldsymbol{C}_s)$	$m'm2'$	$\parallel 2'$	$\perp m$
$\boldsymbol{C}_4$	4	$\parallel 4$	$\parallel 4$
$\boldsymbol{C}_{4v}(\boldsymbol{C}_4)$	$4m'm'$	$\parallel 4$	$\parallel 4$
$\boldsymbol{C}_3$	3	$\parallel 3$	$\parallel 3$
$\boldsymbol{C}_{3v}(\boldsymbol{C}_3)$	$3m'$	$\parallel 3$	$\parallel 3$
$\boldsymbol{C}_6$	6	$\parallel 6$	$\parallel 6$
$\boldsymbol{C}_{6v}(\boldsymbol{C}_6)$	$6m'm'$	$\parallel 6$	$\parallel 6$

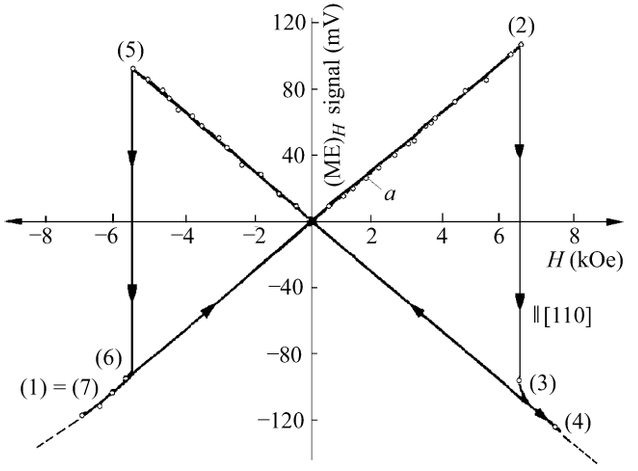

Fig. 1.5.8.2. The hysteresis loop in the linear magnetoelectric effect in ferromagnetoelectric $Ni_3B_7O_{13}I$ at 46 K (Ascher *et al.*, 1966).

Weiss constant. Later, Astrov *et al.* (1968) proved that these compounds undergo a transition into a weakly ferromagnetic state at temperatures $T_N = 11$ and 9 K, respectively.

$BiFeO_3$ is an antiferromagnet below $T_N = 643$ K. This was proved by neutron scattering (Kiselev *et al.*, 1962; Michel *et al.*, 1969) and magnetic measurements (Smolenskii *et al.*, 1962; see also Venevtsev *et al.*, 1987). $BiFeO_3$ also possesses a spontaneous electric polarization. The magnetic point group above T_N is $3m1'$ and below it should have been $3m$ (Kiselev *et al.*, 1962), but in reality it possesses an antiferromagnetic spatially modulated spin structure (Sosnovska *et al.*, 1982). Another ferroelectric antiferromagnet, $YMnO_3$, was found by Bertaut *et al.* (1964). It becomes ferroelectric at $T_c = 913$ K (with paramagnetic point group $6mm1'$) and antiferromagnetic at $T_N = 77$ K. Below this temperature, its magnetic point group is $6'mm'$. The antiferromagnetic ordering was also proved by investigating the Mössbauer effect (Chappert, 1965). The symmetries of both antiferromagnetic ferroelectrics described above do not allow weak ferromagnetism according to Table 1.5.5.2, and, experimentally, a spontaneous ferromagnetic moment has not been observed so far.

Since Schmid (1965) developed a technique for growing single crystals of boracites, these compounds have become the most interesting ferromagnetoelectrics. The boracites have the chemical formula $M_3B_7O_{13}X$ (where $M = Cu^{2+}, Ni^{2+}, Co^{2+}, Fe^{2+}, Mn^{2+}, Cr^{2+}$ and $X = F^-, Cl^-, Br^-, I^-, OH^-, NO_3^-$). Many of them are ferroelectrics and weak ferromagnets at low temperatures. This was first shown for $Ni_3B_7O_{13}I$ (see Ascher *et al.*, 1966). The symmetries of all the boracites are cubic at high temperatures and their magnetic point group is $\bar{4}3m1'$. As the temperature is lowered, most become ferroelectrics with the magnetic point group $mm21'$. At still lower temperatures, the spins of the magnetic ions in the boracites go into an antiferromagnetic state with weak ferromagnetism. For some the ferromagnetoelectric phase belongs to the group $m'm2'$ and for others to $m'm'2$, m', m or 1. In accordance with Table 1.5.8.4, the spontaneous polarization **P** is oriented perpendicular to the weak ferromagnetic moment $\mathbf{M}_D$ for the groups $m'm2'$ and m. There results a complicated behaviour of boracites in external magnetic and electric fields. It depends strongly on the history of the samples. Changing the direction of the electric polarization by an electric field also changes the direction of the ferromagnetic vector (as well as the direction of the antiferromagnetic vector) and *vice versa*.

As an example, Fig. 1.5.8.2 shows the results of measurements on Ni–I boracite with spontaneous polarization along [001] and spontaneous magnetization initially along $[1\bar{1}0]$. A magnetic field was applied along [110] and the polarization induced along [001] was measured. If the applied field was increased beyond 6 kOe, the induced polarization changed sign because the spontaneous magnetization had been reversed. On reversing the applied magnetic field, the rest of the hysteresis loop describing the $ME_{\parallel}$ response was obtained.

If the spontaneous polarization is reversed, *e.g.* by applying an electric field, the spontaneous magnetization will rotate simultaneously by 90° around the polarization axis. Applying magnetic fields as described above will no longer produce a measurable polarization. If, however, the crystal is rotated by 90° around the polarization axis before repeating the experiment, a hysteresis loop similar to Fig. 1.5.8.2 but turned upside down will be obtained (*cf.* Schmid, 1967).

The similarity of the jumps in the curves of linear magnetostriction (see Fig. 1.5.7.2) and magnetoelectric effect in Ni–I boracite is noteworthy. More details about the present state of investigation of the ferromagnetoelectrics are presented in the review article of Schmid (1994*b*).

The ferromagnetoelectrics appear as type 4 and the ferroelectric antiferromagnets of type III^a as types 2 and 3 in Table 1.5.8.3. The table shows that the linear magnetoelectric effect is admitted by all ferromagnetoelectrics and all ferroelectric antiferromagnets of type III^a, except those that belong to the two point groups $\boldsymbol{C}_6(\boldsymbol{C}_3) = 6'$ and $\boldsymbol{C}_{6v}(\boldsymbol{C}_{3v}) = 6'mm'$.

Concluding Section 1.5.8, it is worth noting that the magnetoelectric effect is still actively investigated. Recent results in this field can be found in papers presented at the 1993 and 1996 conferences devoted to this subject (see Schmid *et al.*, 1994; Bichurin, 1997, 2002).

1.5.9. Magnetostriction

The transition to an ordered magnetic state is accompanied by a spontaneous distortion of the lattice, which is denoted spontaneous magnetostriction. The lattice distortion may be specified by the deformation (strain) components S_{ij}. The undeformed state is defined as the crystal structure that would be realized if the crystal remained in the paramagnetic state at the given temperature. This means that it is necessary to separate the magnetostrictive deformation from the ordinary thermal expansion of the crystal. This can be done by measurements of the magnetostriction in external magnetic fields applied in different directions (see Section 1.5.9.2). The magnetostriction arises because the first derivatives of the exchange and relativistic energies responsible for the magnetic order do not vanish at $S_{ij} = 0$. Thus these energies depend linearly on the deformations around $S_{ij} = 0$. That part of the magnetic energy which depends on the deformations (and consequently on the stresses) is called the magnetoelastic energy, $U_{\rm me}$. To find the equilibrium values of the spontaneous magnetostriction, one also has to take the elastic energy into account.

The magnetoelastic energy includes both an exchange and a relativistic part. In some ferromagnets that are cubic in the paramagnetic phase, the exchange interaction does not lower the cubic symmetry. Thus the exchange part of $U_{\rm me}$ satisfies the relations

$$\partial U_{\rm me}/\partial S_{ii} = B_0' \quad \text{and} \quad \partial U_{\rm me}/\partial S_{ij} = 0 \quad (i \neq j). \qquad (1.5.9.1)$$

Such a form of the magnetoelastic energy gives rise to an isotropic spontaneous magnetostriction or volume change (volume striction) which does not depend on the direction of magnetization. In what follows, we shall analyse mainly the anisotropic magnetostriction.

The spontaneous magnetostriction deformations are so small (about 10^{-5}) for some ferro- and antiferromagnets that they cannot be observed by the usual X-ray techniques. However, in materials with ions possessing strong spin–orbit interactions (like Co^{2+}), it may be as large as 10^{-4}. The magnetostriction in rare-